16th World Conference on Earthquake, 16WCEE 2017
Santiago Chile, January 9th to 13th 2017
Paper N° 3622
Registration Code: S-U1464334195

ANALYTICAL CONSIDERATIONS FOR THE DESIGN OF REINFORCED CONCRETE WALLS IN CHILE

L. M. Massone(1), F. Rojas(2), J. I. Alfaro(3), M. Ahumada(3) and A. Hernandez(3)
(1) *Associate Professor, Department of Civil engineering, Universidad de Chile, lmassone@ing.uchile.cl*
(2) *Assistant Professor, Department of Civil engineering, Universidad de Chile*
(3) *Former undergrad student, Department of Civil engineering, Universidad de Chile*

Abstract

Slender rectangular walls with discontinuities at their bases, such as flag walls (setback) or walls with door openings or access, are common in Chilean practice because of the architectural requirements at facades, first floors and underground. Also, the architectural requirements and Chilean idiosyncrasy have forced to the designers to use several wall sections located in a vast area of the floor plan, resulting in many cases in T-shaped walls, with long webs or flanges, which produced large amount of reinforcement in the boundary elements. Many of these types of walls were imposed with large displacement demands in the 2010 Maule earthquake in Chile, and presented flexo-compression failures in the boundary elements, often close to their discontinuities. These observations have shown the need to establish good predictors of compressive or tensile strains in concrete or steel in reinforced concrete shear rectangular with discontinuities and T-shaped walls that leads to limit states or confinement requirements. However, there is limited information about the behavior of such elements, and no designs or guidelines in the current codes consider the effects of discontinuities at the base and the effect of T-shaped walls, especially with long flanges or web.

In this work, a series of analysis that help to incorporate the effect of discontinuities and cross-section, along with different aspect ratios and other considerations in the yield and ultimate curvature, compressive amplification or tensile reduction strains in concrete or steel, and effective flange width for the designs of slender walls are presented, and design recommendations are proposed.

First, the elastic and inelastic components of flexural deformations by means of a fiber model for slender rectangular walls is calibrated and it was found that the elastic component is dependent on the axial load and the boundary steel reinforcement ratio. Additionally, two analytical models are presented that estimate the yield displacement, yield curvature and ultimate curvature of walls with openings, such as flag walls (setback), mainly based on the dimensions of the opening calibrated from a parametric analysis of a non-linear finite element model. The results indicate that these discontinuities can reduce the elastic displacement, due to the presence of a more rigid section above the opening, and in the inelastic component, increasing the strain demands at the base because the opening tends to constrain the plastic hinge within that area. Lastly, in addition of predictors of maximum tensile and compressive strains for T-shaped walls, the effective flange width for different aspect ratios, length of the flange and the web, is studied and compared with actual code recommendation.

Keywords: slender wall; discontinuities; higher modes; shear amplification.

1. Introduction

After the Mw8.8 magnitude earthquake of 2010, observed deficiencies in the wall design prompted a modification of the Chilean standard of reinforced concrete design, which focused on the detailing requirements for the adequate performance of walls. Confinement is incorporated in the boundary elements of walls when the most compressed fiber exceeds a compression strain of 0.003, as required by ACI 318-08 [1] for the building design displacement δ_u. Strains in the most compressed fiber of concrete must not exceed 0.008 [2]. This requirement is determined for an ultimate curvature estimated with **Eq. (1)**, where c is the depth of the neutral axis, h_w is the height of the wall, l_w is the length of the wall, δ_y is the yield displacement, ϕ_y is the yield curvature of the wall, and l_p is the plastic hinge length. **Fig. 1a** shows the scheme of curvature distribution that is consistent with **Eq. (1)**. The actual distribution of curvature usually exhibits a gradual increment within the plastic hinge zone. **Eq. (1)** can be simplified by concentrating all deformation (curvature) within a hinge at the wall base **(Fig. 1b)**.

$$\phi_u = \phi_y + \frac{(\delta_u - \delta_y)}{l_p(h_w - \frac{l_p}{2})} = \frac{\epsilon_c}{c} \leq \frac{0.008}{c} \tag{1}$$

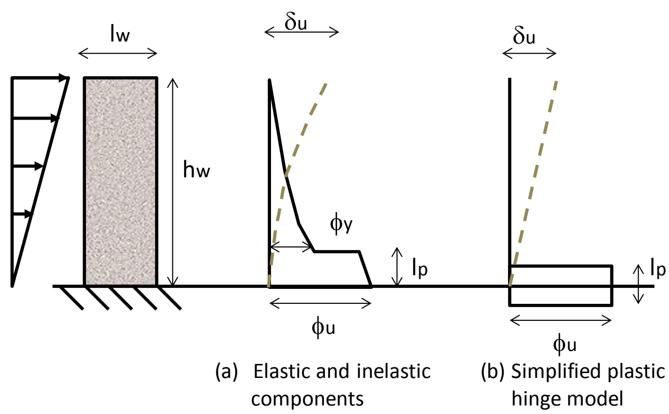

Fig. 1 – Plastic hinge model of wall – (a) Elastic and inelastic components and (b) Simplified plastic hinge model.

Correct estimates of yield displacement and inelastic displacement by means of a plastic hinge model are relevant in modern design of buildings, commonly through wall boundary detailing. It is also important to indicate that many damaged walls had discontinuities at their base, either on the first floor or in the basement, due to clearance or architectural requirements. These discontinuities can be defined as flag-walls or setbacks. This resulted in longer walls towards the terraces or balconies of the apartments on the upper floors (above the first floor or basement), concentrating the damage at the lower level sections. This might indicate that elastic and inelastic component might be different for these types of wall configurations. Additionally, long walls and T-shaped walls are common design, but it is still unclear what reasonable effective widths in such cases are.

2. Model description

The numerical fiber model implemented in OpenSees [3] is a discretization of elements with cross-sections that consist of uniaxial fibers; each element exhibits the mechanical properties of concrete and steel. This first model was used to determine the elastic and inelastic component of rectangular walls.

Another model, based on a membrane element is used for the analysis of walls with discontinuities (flag wall) and T-shaped walls for effective with analysis. The membrane element with layers and degrees of freedom

(DOF) of rotation for the nonlinear analysis of reinforced concrete walls under static and cyclic loadings proposed by Rojas [4] is used. The formulation of the membrane element used in this study is based on a quadrilateral element with 12 DOF, 2 displacements and 1 rotation per node. The element is defined by a mixed interpolation of the displacement element and a layer system that is completely joined to the cross section of the wall, where each layer represents a portion of the wall (cover concrete, confined concrete, steel mesh).

3. Elastic curvature and displacement of walls – rectangular wall

The two main parameters required for the analysis are the yield curvature (ϕ_y) and the yield displacement (δ_y). In both cases, the first yield is used. The first yield top displacement $\delta_y = \alpha \phi_y {h_w}^2$ can be calculated for a triangular lateral load pattern from a model that assumes a variable stiffness to the top of the structure. The yield curvature can be calculated as $\phi_y = \frac{\epsilon_y}{\xi l_w} = K\frac{\epsilon_y}{l_w}$. The section geometry, the distribution of cracking over the height, the level of axial load, the boundary reinforcement and other considerations affect the yield curvature and the yield displacement, which are reflected in coefficients α and K, and are investigated.

In the analysis, the variables are defined as follows: wall length of 2.5 m, 5 m, and 7.5 m are considered, axial load of $0.1f'_cA_g$, $0.2f'_cA_g$, and $0.3f'_cA_g$ are included, and regarding the boundary reinforcement ratio (over the boundary cross-section) a broad range of values is considered, although values between 5% and 6% are more frequently observed in buildings in Chile [5].

In this analysis, the variables with the greatest impact on the yield curvature are the axial load and the amount of boundary reinforcement. The factor K can be parameterized in terms of these two variables, as $K = 1.25 + 1.69\frac{P}{f'_cA_g} + 0.65\rho_b$. Based on the results, a conservative value of K = 1.4 can be considered for a boundary reinforcement ratio over 5% and axial loads over $0.1f'_cA_g$. The variable α is dependent on the amount of boundary reinforcement. The α-values were calculated as $\alpha = 0.33{\rho_b}^{0.14}$. α = 0.22 is a conservative value for walls with a boundary reinforcement ratio larger than 5%. More details can be found in Massone and Alfaro [6].

4. Inelastic displacement component – rectangular wall

Eq. (1) can be used to estimate the curvature demands (or strains in the most compressed boundary wall) after the elastic limit is exceeded. Simplified expressions, such as **Eq. (2)**, have been used to determine confinement requirements in design (e.g., ACI 318-08 [1]; Moehle [7]) based on a hinge at the base of the wall, where all curvature is represented by an equivalent rectangle (**Fig. 1b)**. A hinge length of $0.5l_w$ is a common assumption.

$$\phi_u = \frac{\delta_u}{h_w l_p} \tag{2}$$

The plastic hinge length has been studied by several authors, including Paulay and Uzumeri [8], who adapted an equation that was proposed for beams for walls. Other expressions have incorporated effects such as shear, strain penetration [9] or the level of axial load [10]. Regarding the axial load, Bohl and Adebar [10] investigated the dependency of the plastic hinge length to the axial load from a finite element model, resulting in **Eq. (3)**, which is limited to 0.8 l_w. The analysis was primarily performed for roof drift levels of 2%. In **Eq. (3)**, the variable z recognizes that the plastic hinge length is impacted by the moment-shear ratio at the plastic hinge location, assumed at the wall base ($z = M/V$).

$$l_p = (0.2l_w + 0.05z)(1 - \frac{1.5P}{f'_cA_g}) \tag{3}$$

Other parameters that may impact the wall response include hardening of the reinforcement, the amount of boundary reinforcement and the inelastic roof drift level. To examine the impact of these variables, a numerical nonlinear analysis of the implemented models is performed.

Generally, the plastic hinge length $l_p = 0.5{l_p}^*$, where ${l_p}^*$ is the distance from the wall base to the point at which the yield strain is attained in the reinforcing bar that is subjected to tension. Therefore, the equivalent rectangle for plastic curvatures is consistent with a linear distribution of plastic curvature over ${l_p}^*$. For consistency in this study, ${l_p}^*$ is defined for the first yield, tracking yielding in the extreme tensile reinforcement along the height of the wall. From the results of the numerical analysis, a regression was performed to modify the expression proposed by Bohl and Adebar [10], as shown in **Eq. (4)**. The analysis results indicate that the plastic hinge length increases with the level of plastic displacement or drift $\Delta_p = \frac{(\delta_u - \delta_y)}{h_w}$ instead of the total drift, starting from zero plastic hinge length at zero plastic drift, which is consistent with the inexistence of inelastic deformation [6].

$$l_p = (0.2l_w + 0.05z)(1 - \frac{1.5P}{f'_c A_g})(6.7{\Delta_p}^{0.3}) \tag{4}$$

A correct estimate of the plastic hinge length does not guarantee a correct estimate of the curvature demand. The behavior of steel is highly relevant in the curvature at the wall base and the distribution over height [6, 11]. Thus, the effect of the steel behavior on the distribution of curvature along the height is examined. In order to capture the curvature distribution, a modified expression of **Eq. 1** for the ultimate curvature is proposed (**Eq. 5**). The new expression considers an inelastic nonlinear curvature distribution of the type $\phi(y) = (\phi_u - \phi_y)\left(\frac{y}{l_p^*}\right)^{(2/\beta-1)} + \phi_y$, where y is measured along the height of the wall from the yield point to the bottom and β is a parameter related to the way the curvature increases (in general, β<1 and β=1.0 for linear distribution). Considering that $h_w \gg \frac{l_p}{2}$ in tall buildings, the expression for the ultimate curvature reduces to,

$$\phi_u = \phi_y + \frac{(\delta_u - \widetilde{\delta_y})}{\beta l_p \left(h_w - \frac{l_p}{2}\right)} \tag{5}$$

This expression also includes a correction of the yield displacement component δ_y determined at first yield. The corrected yield component ($\widetilde{\delta_y}$) is calibrated as $\widetilde{\delta_y} = \delta_y \left[1 + 0.9\left(\frac{l_p}{h_w}\right)^{0.23}\right]$. Generally, $\widetilde{\delta_y} \approx 1.4\delta_y$. Parameter β is dependent on the onset of hardening (ε_{sh}) and the post-yield relative stiffness (b), as well as the boundary reinforcement ratio (ρ_b), assuming that the web-distributed reinforcement is less representative. **Eq. (5)** and **(6)** together are capable of predicting the variation of curvature.

$$\beta = 10(b\rho_b)^{0.42}(1 - (\varepsilon_{sh} - \varepsilon_y)^{0.22}) \tag{6}$$

In **Fig. 2a,** the estimation of the curvature (**Eq. 5**) versus the curvature obtained from the analysis (fiber model) is shown for the same cases examined for the plastic hinge length. Additionally, the ultimate curvature is also estimated from **Eq. (2**), which considers the plastic hinge length $l_p = l_w/2$ (**Fig. 2b**). The data are separated into two groups: the first group (solid symbols) covers roof displacements less than or equal to $1.5\%\frac{N}{20}$ with N number of floors; the second group (empty symbols) considers higher levels of lateral displacements. In **Fig. 2a**, the estimated average curvature values are similar to the values obtained from the numerical analysis with a mean value of 0.99 and a dispersion of 0.28. **Fig. 2b** shows that **Eq. (2)** is more conservative in general (avg=1.8) in estimating the ultimate curvature but has a large dispersion (sd=1.35), which indicates that it is not conservative for an important number of cases.

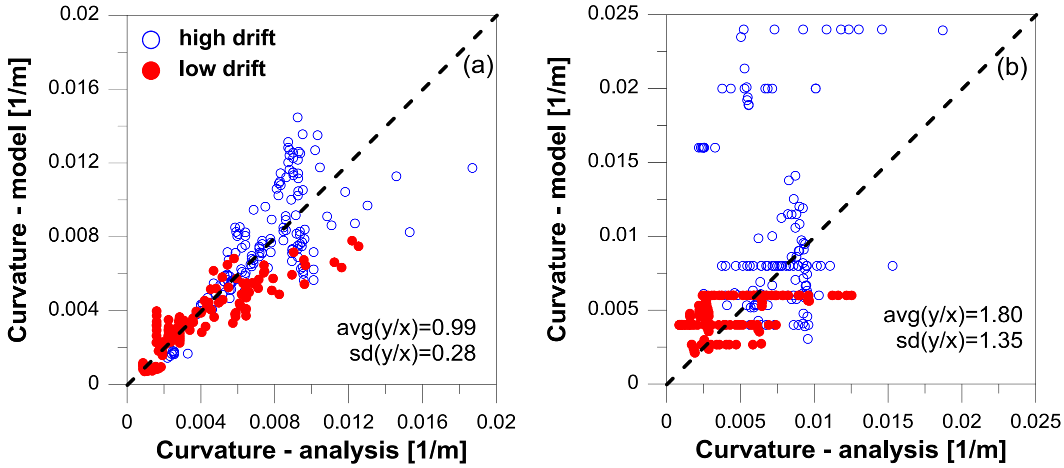

Fig. 2 – Curvature prediction versus analysis: (a) proposed model and (b) simple plastic hinge [6].

5. Curvature distribution - flag wall

The parametric study of flag-wall is primarily characterized by the change of sections (increased of wall length) of a certain height. This is one of the most common types of discontinuity in Chilean buildings, where most of the damage in RC buildings during the Mw8.8 earthquake of 2010 [12, 13] was observed.

Thirteen cases of flag-walls were analyzed (**Fig. 3**). Details of specimen characteristics can be found in Ahumada [14]. In these models, the curvature profile over the wall height was studied, as was the distribution of plasticity (height at which yielding is observed in the most tense fiber), and compared with a rectangular wall that had a length equal to the length of the wall at the base of the discontinuity. For the cases under analysis, a simplified version based on the flexural behavior only was considered since the curvature was little affected. This model was obtained by placing horizontal rigid beams at all levels. The following parameters were varied: length of discontinuity (l_x), longitudinal boundary steel ratio (LSR), aspect ratio (AR) relative to the total wall length (l_w) with a constant opening height (h_x) and total wall length (l_w).

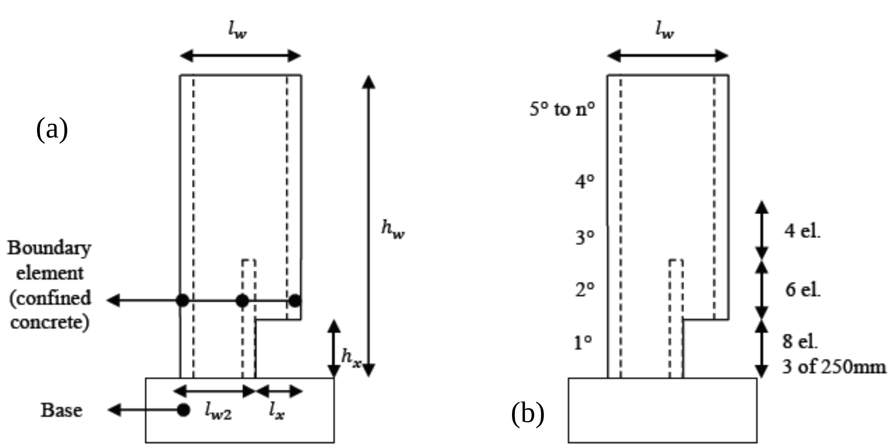

Fig. 3 – Flag-walls – (a) Distribution of longitudinal reinforcement, (b) discretization (mesh).

When comparing the behavior of rectangular walls with that of walls with discontinuities at the base, two interesting phenomena are observed: (1) early yield and (2) the concentration of plasticity. To study the yield displacement, the first yield is defined as the moment (or displacement) at which the wall fiber with the largest tensile strain at the base yields (reaching the level of apparent yield). The analysis shows that for the walls with discontinuity, the first yield occurs early (at a lower drift level) compared with rectangular walls. This effect is enhanced if the length of the opening increases relative to the length of the wall and is more significant with a larger aspect ratio of the wall. In **Fig. 4**, this effect is shown, where the initiation of yielding begins with the wall with an opening. The figure shows the results of flag walls with l_w = 5 m, and 2 cases of reduced section at the base l_x/l_w = 0.2 and 0.4. In the case of rectangular walls, in order to compare the response to the flag walls, the wall length was set equal to the reduced section at the base (l_{w2} = 3, 4 m, comparable with flag-walls with l_x/l_w = 0.4 and 0.2, respectively).

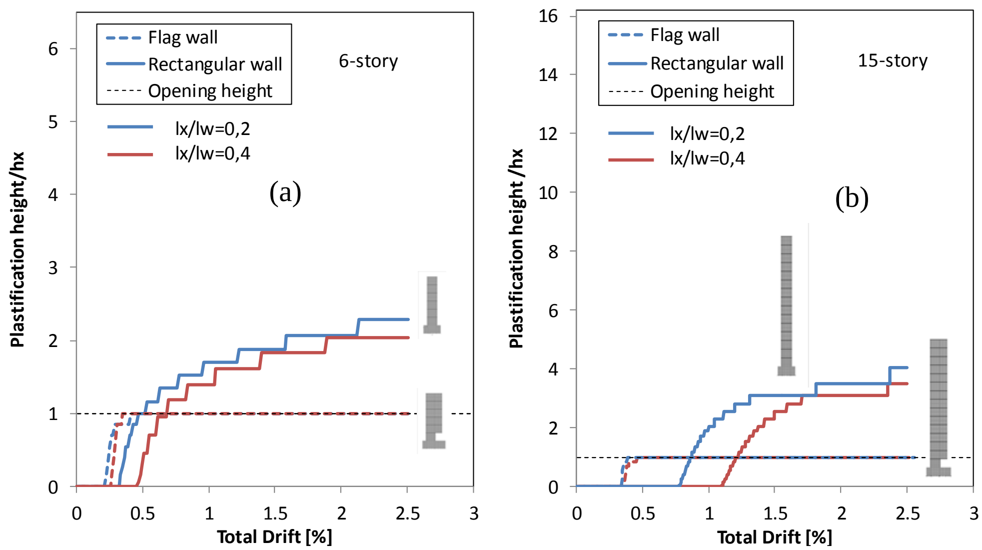

Fig. 4 – Plastification distribution versus drift for (a) 6-story buildings and (b) 15-story buildings with discontinuity length of 20% and 40% of the wall length.

Fig. 4 also shows the height at which the longitudinal reinforcement has reached yielding by pointing out the instant (drift) where an extreme fiber yields for walls of 6 and 15 floors, representing the distribution zone of the plastification in height. In comparing the rectangular wall with the discontinuous wall, for the latter, plastification tends to stagnate once it reaches the level of the discontinuity, suggesting that the entire top section of the wall (longer section) behaves more rigidly than does the base of the wall. This phenomenon occurs for all analyzed opening sizes (width and height) and is more noticeable in walls with greater height, which is explained by the fact that the area of rectangular wall plastification partly increases with height; conversely, in the flag-walls, plasticity concentrates at the wall base because of the greater rigidity of the upper section.

For an idea of what occurs with the strains in both the discontinuous and continuous area, **Fig. 5** shows the curvature values of numerical models in each element for the walls considered, comparing a rectangular and a discontinuous wall. In the figures, the negative quadrant represents the curvature distribution obtained for the rectangular wall, and the positive quadrant shows the same information for the discontinuous wall. Models for $l_x = 0.2l_w$ and $l_x = 0.4l_w$ (left and right figures, respectively) are shown, as are models for walls with 6 and 15 floors (top and bottom figures, respectively), consistent with $h_x = 0.17h_w$ and $h_x = 0.067h_w$, respectively. The height of the opening is fixed at the floor height such that the relative height (h_x/h_w) of the opening decreases with increasing number of floors. The curvatures tend to concentrate in the area of the opening, which explains the tendency to limit the area of the plastification in the opening. The strain values above the opening are not significant compared with the strain values under the opening. The length of the opening is not relevant to this effect because for both lengths (l_x/l_w=0.2 and 0.4), the curvature is concentrated at the base. Furthermore, a low ratio of the opening height and the wall (h_x/h_w) has a significant effect on the concentration of the base curvature.

This finding suggests that a rectangular plastic hinge type of model concentrated at the base is adequate to quantify the ultimate curvature values in cases with relatively low opening heights.

The significant increase in the compressive strain (the strain can easily double its value) suggests that both a reduction of the elastic deformation and increased strains by concentrating the curvature in the opening area should be considered when detailing reinforced concrete flag-walls.

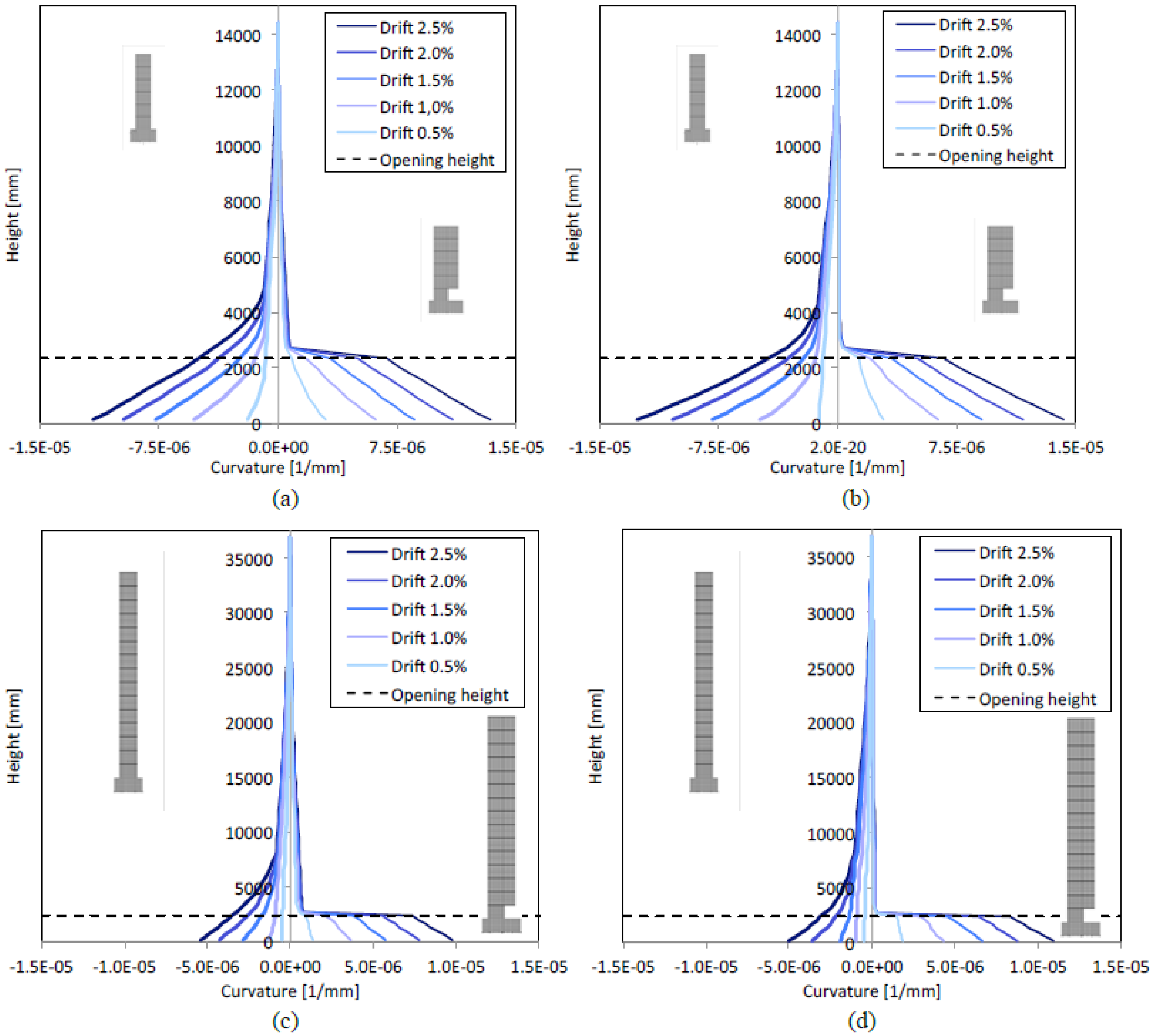

Fig. 5 – Wall curvature distribution for rectangular and flag-wall, a) 6 floors, l_x/l_w=0.2, b) 6 floors, l_x/l_w=0.4, c) 15 floors, l_x/l_w=0.2 and d) 15 floors, l_x/l_w=0.4.

6. Effective flange width for T-shaped walls

In the design and detailing of reinforced concrete walls, some assumptions are used, such as the effective flange width, which current design code considered valid for non-rectangular cross sections with significant long flanges and different aspect ratios.

The effective flange width is defined as the portion of the flange of the cross section of for example a T-shaped wall (see **Fig. 6a**), which resist the action of lateral loads acting in the direction of the web of the wall. **Figure 6a** shows how the stress decreases from the flange-web intersection to the edges of the flange, where the farthest reinforcement has low effectiveness.

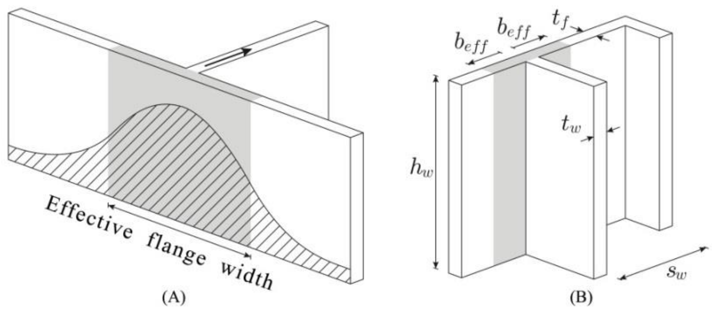

Fig. 6 – Stress distribution to the tension flange and defining effective width.

Several authors and design codes have proposed expressions for the effective flange width (b_{eff}) depending on the height of the wall, flange thickness, among others (see **Fig. 6b**). For example, the ACI 318-08 [1] proposes that the effective flange width is given as a function of the wall height (h_w) or the free distance to the web of an adjacent wall (S_w) as the minimum of $0.25h_w$ and $S_w/2$, while the Japanese Code [15], relates the effective flange width to the thickness of the flange, as the minimum of $6t_f$ and $S_w/4$.

To study the effective flange width, a parametric study is performed, with various sizes of T-shaped walls and aspect ratios (h_w / l_w) varying from 3 to 9, with 2% of steel ratio at the boundary of the wall and under a constant axial load of $0.1f_c'A_g$. In this study, the shell element developed by Rojas [4] is used. The different T-shaped wall geometric sections used in this study are presented in **Fig. 7**. The length of the flange of T2 and T3 walls are two and four times the size of T1, respectively. However, T4 has a web two times larger than T1. Furthermore, in T2B and T3B cases, longitudinal reinforcement distributed along the flange is incorporated with the same steel ratio of the flange boundary element of T2A and T3A, respectively, as shown in grey in the figure. More details can be found in Hernández [16].

To evaluate the effective flange width, the following expression is proposed:

$$b_{eff} = \frac{\sum f_i \, w_i}{max(f_{fw})} \tag{7}$$

The expression is based on the calculation of the average stress of the reinforcement across the flange, where f_i is the stress in the reinforcement at the quadrature point i of each shell element, derived from the stress-strain relationship of the reinforcement, w_i is the contribution width of the quadrature point and f_{fw} is the maximum stress of the reinforcement in the flange (typically at flange-web intersection). It is decided to normalize the expression by the maximum stress of the flange, because the stress of the reinforcement in the flange could be greater than f_y after yielding. **Fig. 8** shows the effective flange width normalized by the total length of the flange (LF). In all cases, there is a rapid increase in the effective flange width after first yielding in the flange. Also, the drift when occurs the first yield increases with the aspect ratio (AR). For example, first yielding occurs at a drift of 0.5% for an aspect ratio of 3 compared to a drift of 1.25% for an aspect ratio of 9. As it can be seen, if yielding is expected in the flange, the effective length is at least 0.6LF, however, relatively small increments of drift result in yielding of the entire flange, which makes the entire section effective for design or detailing purposes.

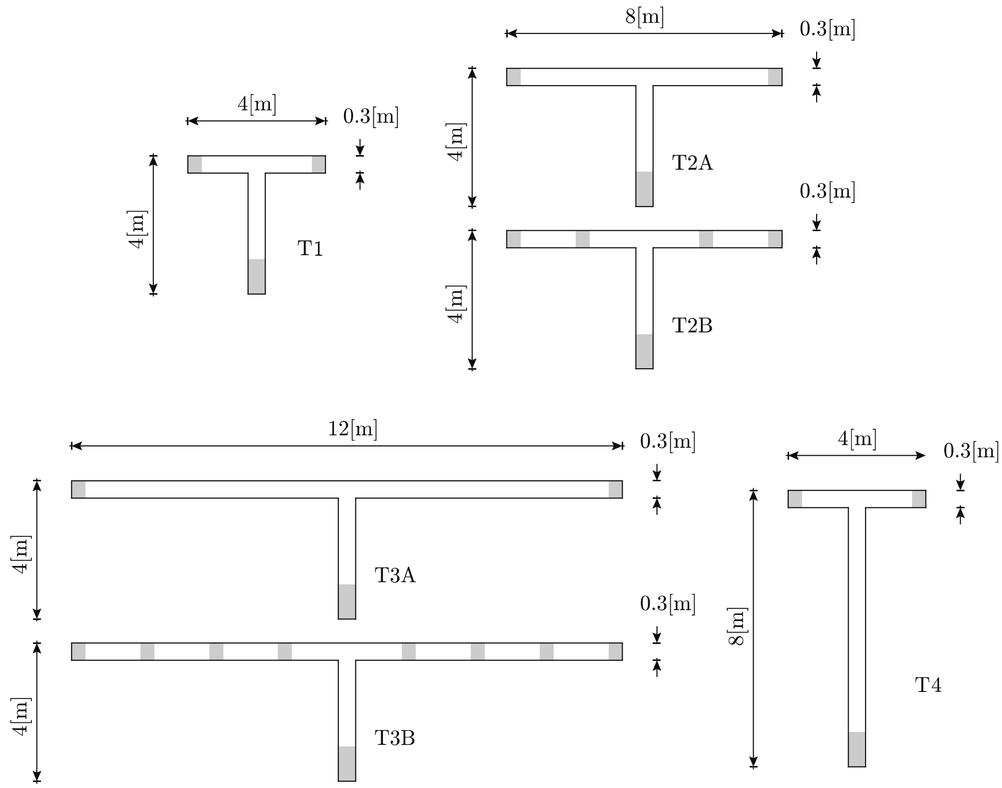

Fig. 7 – Geometric sections of the walls with section T.

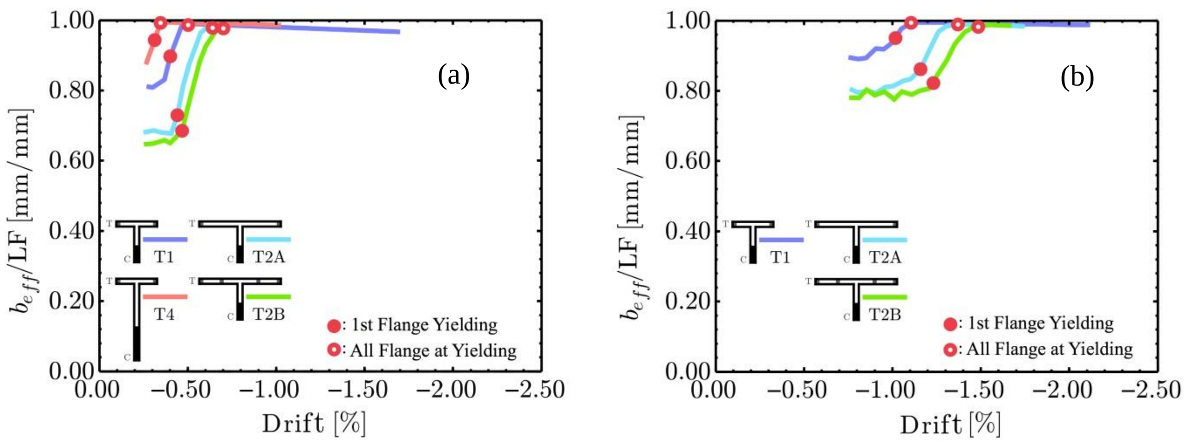

Fig. 8 – Effective width normalized by flange length (LF) for an aspect ratio of (a) 3 and (b) 9.

7. Conclusions

A series of monotonic analyses of rectangular walls with a triangular lateral load distribution that considers different variables, such as axial load and the amount of boundary reinforcement, are performed. From these analyses, an expression that estimates the yield curvature (related to K) is determined based on axial load and boundary reinforcement. However, a conservative value of K = 1.4 can be used. An analytical expression based on parameter α for estimating the yield displacement, which is dependent on the amount of boundary reinforcement, is calibrated. Based on the numerical analysis, $\alpha = 0.22$ can be conservatively assumed.

The inelastic response is used to calibrate an expression for the plastic hinge length. A set of numerical analyses are conducted considering several variables, such as axial load, wall length and height, and drift level. Incorporating the plastic drift (Δ_p) attained by the wall improves the estimation of the plastic hinge length.

A parametric analysis is then implemented to describe the behavior of walls with openings at the base, which is defined as a section reduction or flag-wall. The distribution of curvature along the height of the wall for different drift levels for the elastic and plastic range is studied. The walls with openings at the base with relative heights less than 20% of the wall height tend to develop a concentration of curvature over the entire height of the section with the reduced section, which are more significant in the elastic range and cause a considerable reduction of deformation in the upper section (larger). This behavior results in a yield displacement for the flag-wall that develops earlier compared with that of the rectangular wall (with same section as the base of the discontinuous wall), and the ultimate curvature is increased for the same drift level.

The study of the effective flange width, that is required for detailing when the flange is in tension, indicates that is it could be as low as 0.6LF for a wall with an aspect ratio of 3 (increases with the aspect ratio) once yielding starts, however, relatively small increments of drift results in yielding of the entire flange making it fully effective.

8. References

[1] ACI 318-08. 2008. Building Code Requirements for Structural Concrete and Commentary. Committee 318. American Concrete Institute, Farmington Hills, Michigan.

[2] Massone LM. 2013. Fundamental principles of the reinforced concrete design code changes in Chile following the Mw8.8 earthquake in 2010. Engineering Structures. 56:1335-1345.

[3] OpenSees. 2000. http://opensees.berkeley.edu/.

[4] Rojas F. 2012. Development of a nonlinear quadrilateral layered membrane element with drilling degrees of freedom and a nonlinear quadrilateral thin flat layered shell element for the modeling of reinforced concrete walls. PhD Dissertation, University of Southern California, California.

[5] Estay C. 2008. Characteristics of Reinforced Concrete Wall Design in Chile (in Spanish). Civil Engineering Thesis. School of Engineering. University of Chile.

[6] Massone LM, Alfaro JI. 2016. Displacement and curvature estimation for the design of reinforced concrete slender walls. Struct. Design Tall Spec. Build. DOI: 10.1002/tal.1285 (in press).

[7] Moehle JP. 1992. Displacement-Based Design of RC Structures Subjected to Earthquakes. Earthquake Spectra. 8(3):403-428.

[8] Paulay T, Uzumeri SM. 1975. A Critical Review of the Seismic Design Provisions for Ductile Shear Walls of the Canadian Code. Canadian Journal of Civil Engineering. 2:592-601.

[9] Hines EM, Restrepo JI, Seible F. 2004. Force-displacement characterization of well-confined bridge piers. ACI Structural Journal. 101(4):537–548.

[10] Bohl A, Adebar P. 2011. Plastic Hinge Lengths in High-Rise Concrete Shear Walls. ACI Structural Journal. 108(2):148-157.

[11] Dazio A, Beyer K, Bachmann H. 2009. Quasi-static cyclic tests and plastic hinge analysis of RC structural walls. Engineering Structures. 31(7):1556–1571.

[12] Wallace JW, Massone LM, Bonelli P, Dragovich J, Lagos R, Lüders C, Moehle J. 2012. Damage and Implications for Seismic Design of RC Structural Wall Buildings. Earthquake Spectra. 28(S1):S281-S299.

[13] Rojas F, Naeim F, Lew M, Carpenter LD, Youssef NF, Saragoni GR, and Schachter MA. 2011. Performance of tall buildings in Concepcion during the 27 February 2010 moment magnitude 8.8 offshore Maule, Chile earthquake. The Structural Design of Tall and Special Buildings, 20(1):37–64.

[14] Ahumada M. 2014. Finite Element Modeling of Slender Walls with Discontinuities. Design Recommendations (in Spanish). Civil Engineering Thesis. University of Chile.

[15] Architectural Institute of Japan. 2010. AIJ Standard for Structural Calculation of Reinforced Concrete Structures (in Japanese).

[16] Hernández A. 2015. Bernoulli Hypothesis Verification in Reinforced Concrete Wall Sections (in Spanish). Civil Engineering Thesis. University of Chile.